



HAL
open science

Upper mantle structure beneath continents: New constraints from multi-mode Rayleigh wave data in western North America and southern Africa

Sophie Merrer, Michel Cara, Luis Rivera, Jeroen Ritsema

► To cite this version:

Sophie Merrer, Michel Cara, Luis Rivera, Jeroen Ritsema. Upper mantle structure beneath continents: New constraints from multi-mode Rayleigh wave data in western North America and southern Africa. *Geophysical Research Letters*, 2007, 34 (6), 10.1029/2006GL028939 . hal-03202458

HAL Id: hal-03202458

<https://hal.science/hal-03202458>

Submitted on 20 Jul 2021

HAL is a multi-disciplinary open access archive for the deposit and dissemination of scientific research documents, whether they are published or not. The documents may come from teaching and research institutions in France or abroad, or from public or private research centers.

L'archive ouverte pluridisciplinaire **HAL**, est destinée au dépôt et à la diffusion de documents scientifiques de niveau recherche, publiés ou non, émanant des établissements d'enseignement et de recherche français ou étrangers, des laboratoires publics ou privés.

Copyright



Upper mantle structure beneath continents: New constraints from multi-mode Rayleigh wave data in western North America and southern Africa

Sophie Merrer,¹ Michel Cara,¹ Luis Rivera,¹ and Jeroen Ritsema²

Received 29 November 2006; revised 1 February 2007; accepted 23 February 2007; published 28 March 2007.

[1] We estimate the averaged 1-D shear-wave velocity of the upper mantle beneath western North America and the Kaapvaal region in southern Africa by inverting dispersion measurements of fundamental and higher Rayleigh modes recorded by ~ 2000 km aperture broadband arrays. The overtones at periods exceeding 25 s constrain the averaged 1-D shear-wave velocity to 650 km depth across the regional arrays. Our overtone analysis confirms the shear-wave velocity differences observed in global tomographic models with similar horizontal resolution: the western North American mantle features a prominent low velocity zone at depths 50–200 km, while the shear velocity in the upper 180–200 km of the mantle beneath southern Africa is at least 6% higher than in western North America which we interpret as the expression of a cratonic keel. There is no resolvable difference in shear-wave velocity between southern Africa and western North America below a depth of about 300 km. **Citation:** Merrer, S., M. Cara, L. Rivera, and J. Ritsema (2007), Upper mantle structure beneath continents: New constraints from multi-mode Rayleigh wave data in western North America and southern Africa, *Geophys. Res. Lett.*, *34*, L06309, doi:10.1029/2006GL028939.

1. Introduction

[2] Surface-wave seismology is a powerful tool to investigate the shear velocity structure of the upper mantle. Most regional surface-wave studies rely on fundamental mode observations only, while it is well known that the use of overtone surface waves may greatly improve the depth resolution of shear velocity below 200–300 km depth. It is difficult to analyze these overtones because, over an important range of periods, they propagate with similar group velocities. Furthermore, relatively deep (>50 km) or large crustal earthquakes are required to excite overtone signals so they can be well recorded. While new methods such as the continuous wavelet transforms [Holschneider *et al.*, 2005] improve the time-frequency resolution in fundamental mode surface wave analysis, they do not address how the analysis of interfering overtone signals can be improved. Waveform inversion techniques [e.g., Woodhouse and Dziewonski, 1984; Nolet, 1990; Debayle *et al.*, 2005] rely on fewer independent pieces of information than those based on the measurements of individual overtone disper-

sion. A decomposition of a waveform into a set of individual modes through a set of secondary observables, as done for example by Debayle *et al.* [2005], is intrinsically non unique and provide less information than the kind of data we present here.

[3] It is straightforward to isolate the individual modes by wavenumber domain analysis when data from arrays of seismic stations are available. Techniques based on this approach were developed by Nolet [1975] and Cara [1976] more than three decades ago and these authors demonstrated their robustness with applications to analog WWSSN seismograms. Nowadays, regional arrays of broadband, high-dynamic range stations are in operation worldwide, allowing us to apply these established techniques to much higher quality data.

[4] In this paper, the phase-velocities of fundamental mode and up to the fourth overtone Rayleigh waves (period $T > 25$ s) are measured by U-C diagram analysis [Cara, 1976, Cara and Minster, 1981] and inverted for 1D shear velocity profiles. We use regional network data from western North America (WNA) and the Kaapvaal Craton (KC) region in southern Africa which can be regarded as end-member tectonic regions: a young active tectonic province with subducted oceanic ridges and an old stable continental region. The stations in WNA comprise a selection of the Berkeley Digital Seismic Network (operated by UC Berkeley), TriNet (Southern California Seismic Network operated by Caltech and the USGS), and the NARS-Baja array [Trampert *et al.*, 2003] stations. Stations in the KC region are from the SASEK-Kaapvaal network [Carlson *et al.*, 1996]. The SASEK network has a dense station spacing but recordings are generally noisier than the recordings from our selection of WNA stations. Unfortunately, only four deep earthquakes at suitable azimuths were recorded during the deployment of the SASEK array so the KC data set is of somewhat lower quality than WNA data.

2. The U-C Diagram Technique

[5] The U-C Diagram technique is aimed at measuring the phase velocity dispersion of interfering surface wave modes. It is based on the assumption that, at a fixed period T_n , different modes “ p ” have group velocities close to a reference value, but different phase velocities. Ideally, the method is applied to seismograms from an array of stations at a common source azimuth (Figure 1, top). After narrow-band filtering around a period T_n , the records are first phase and time shifted according to a trial phase velocity C and the reference group velocity, and are then stacked. The U-C diagram displays the envelopes of the waveform stacks as a function of C and group velocity U , for each period T_n

¹Institut de Physique du Globe de Strasbourg, CNRS and Université Louis Pasteur, Strasbourg, France.

²Department of Geological Sciences, University of Michigan, Ann Arbor, Michigan, USA.

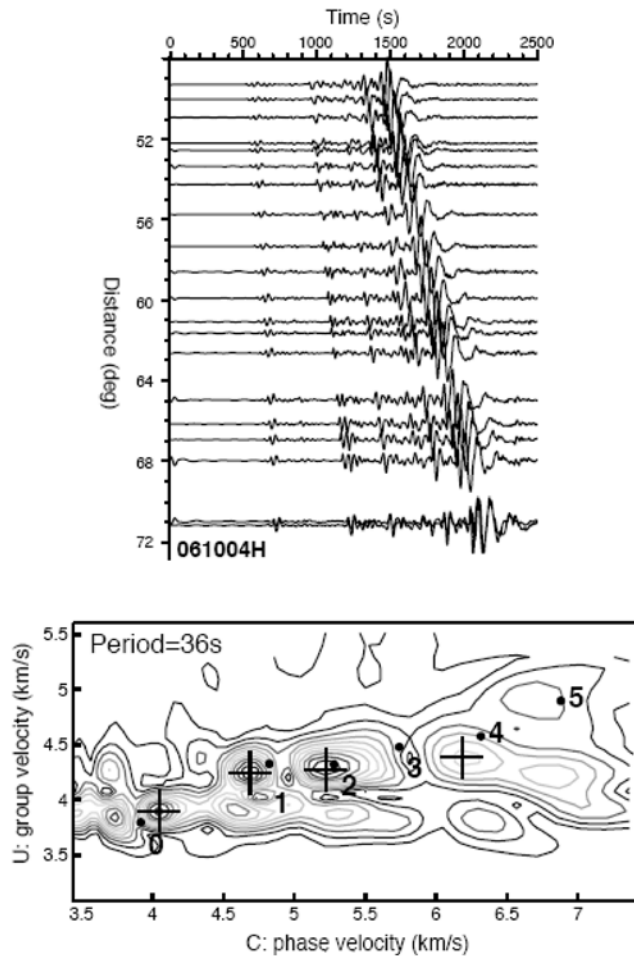


Figure 1. (top) Vertical component recordings of the June 6, 2004 Kamchatka earthquake (depth = 188 km; $M_w = 6.8$) at stations in western North America. (bottom) U-C diagram (for a period $T_n = 36$ s) computed for the same event. The diagram shows the amplitude of the stacked phase and time shifted complex signals versus two axes: the trial phase velocity C and the group velocity U . Contours spacing is 10% of the maximum amplitude. Black circles indicate the theoretical U-C (group and phase velocity) values of the fundamental mode (0) and the first five (1–5) overtones which are computed for the crust-adapted PREM model. Crosses indicate the observed values (mode 0, 1, 2 and 4).

(Figure 1, bottom). Maxima in the stacks are associated with Rayleigh modes p with phase and group velocities $C_p(T_n)$ and $U_p(T_n)$, respectively.

[6] Phase velocity resolution is determined by the aperture of the array and inter-station spacing must be small enough to minimize aliasing effects [e.g., *Cara and Minster, 1981*]. The aperture of the WNA and KC arrays are 2200 km and 1900 km, respectively. To estimate uncertainties in the phase velocity measurements, we calculate U-C diagrams for synthetic seismograms for a crust-adapted PREM model [*Dziewonski and Anderson, 1981*] and Centroid Moment Tensor source parameters (www.globalcmt.org) and invoke the same processing parameters used in the analysis of real data. We identify the modes by visual inspection. We consider the differences between the phase

velocities inferred from the synthetic U-C diagrams and the theoretical values as minimum measurement errors since we do not account for (potentially larger) errors due to noise, Rayleigh wave multi-pathing, or U-C diagram misinterpretation. The rms of these differences were used as a priori errors of the phase velocity measurements in the inversion for shear velocity.

3. Observed Phase Velocities and Inversion

[7] For analysis of the WNA region, we have selected 14 earthquakes with a magnitude larger than 6 in the northwest Pacific region and South America (Figure 2, top). Nine of these earthquakes occurred at 180 km or greater depth and rendered excellent Rayleigh wave overtone recordings. Because considerable waveform complexity appears in the fundamental-mode signals for some of the Northwest Pacific earthquakes, possibly due to lateral refraction and

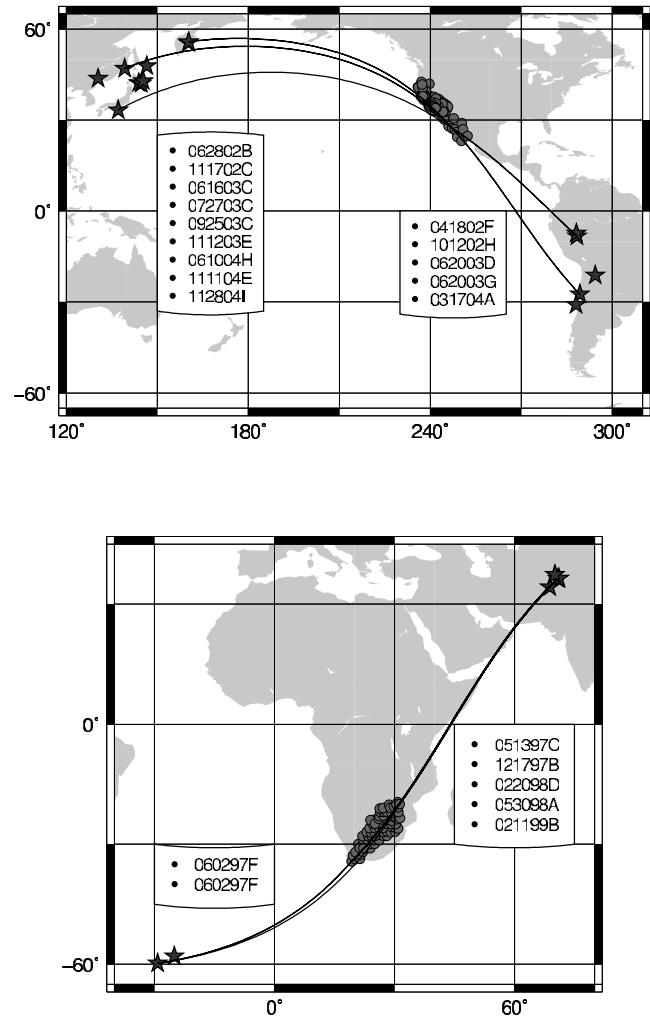


Figure 2. (top) Epicenters of the earthquakes selected for the study of Western North America and great circle paths toward California. (bottom) Epicenters of the events selected for the study of the Kaapvaal craton and great circle paths toward the Kaapvaal network. Harvard code numbers of the different earthquakes are indicated in the inserts.

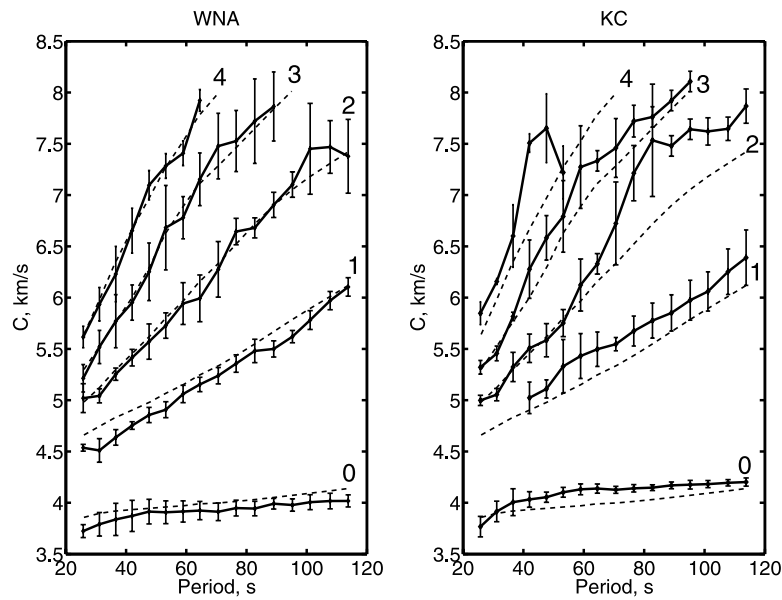


Figure 3. Absolute phase-velocities inferred from the U-C diagrams (solid line) and theoretical values computed for a reference shear velocity model (smoothed PREM) (dashed line) for mode 0 through 4, WNA for western North America and KC for the Kaapvaal region. Error bars are rms estimated from synthetic experiment.

mode conversions when Rayleigh waves propagate along the continental margin of California, we measure fundamental-mode Rayleigh wave dispersion using South American earthquake recordings only. For analysis of the KC region, we have collected data for 7 earthquakes in the South Sandwich Islands and the Hindu Kush and Afghanistan-Tajikistan border regions (Figure 2, bottom). Four of these earthquakes are deep. The phase-velocity measurements for periods longer than 25 s and the standard errors estimated from synthetics are displayed in Figure 3.

[8] We invert the phase velocity data assuming linear isotropic shear-wave velocity perturbations following the formulation by *Tarantola and Valette* [1982], Gaussian statistics as in work by *Lévêque et al.* [1991], and partial derivatives $\partial C_p(T_n)/\partial V_s(z)$ according to *Takeuchi and Saito* [1972]. According to our experience with similar data, the a priori standard deviations of the shear-wave velocities are fixed to 0.05 km/s and the vertical correlation length to 50 km as in *Debayle and Lévêque* [1997]. The starting model is a smoothed PREM without upper-mantle discontinuities to minimize the effects of a priori constraints in the inverted shear-wave velocity model [*Sieminski et al.*, 2003]. Figure 4 shows the best-fitting shear velocity profiles for the WNA and KC regions and a posteriori error estimates.

[9] To 200 km depth, the WNA and KC shear-wave velocity profiles reveal differences up to 6%. This contrast is about half the 10–15% contrast inferred from global 3D overtone Rayleigh wave models [e.g., *Ritsema et al.*, 2004], or from the regional WNA and KC models reconstructed from the global 3D models of *Debayle et al.* [2005]. Our KC shear-wave velocities are close to the SV part of the anisotropic KA1 model of *Freybourger et al.* [2001] above 100 km depth but are slower below and are also slower than the 1-D southern Africa model from *Li and Burke* [2006] between 40 and 150 km. One reason for this is a paradoxically rather low depth-resolution in the upper part of our

model, mainly due to the small relative weight of fundamental versus overtone dispersion data. Indeed, most of the information constraining the upper 200 km of the model comes from the fundamental and the first overtone as it can be seen by confining the inversion to the modes 0 and 1 (Figure 5). Better quality fundamental mode data would be required to constrain the model above 150 km depth. At greater depths beneath southern Africa, we find a low velocity minimum around depths 180–200 km with veloc-

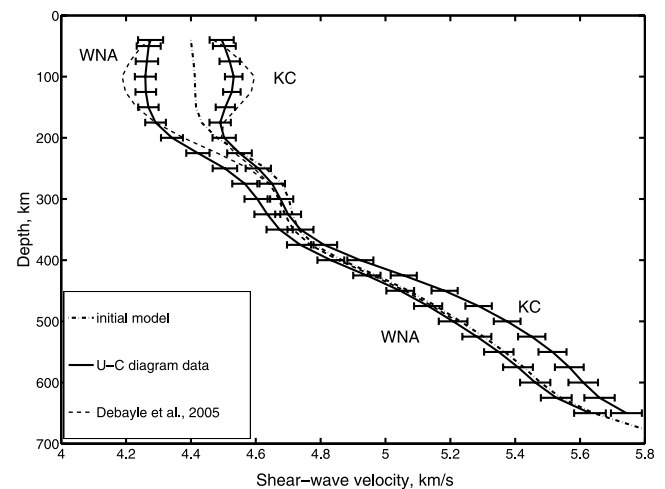


Figure 4. Western North America (WNA) and Kaapvaal Craton (KC) shear velocity profiles (solid lines) and a posteriori errors obtained from the inversion of the phase velocity data from Figure 3. The common starting shear velocity model is shown with a dashed-dotted line. The dashed lines indicate the average WNA and KC shear velocity structure computed from the 3D global model of *Debayle et al.* [2005]. This 3D model is based on the same starting model.

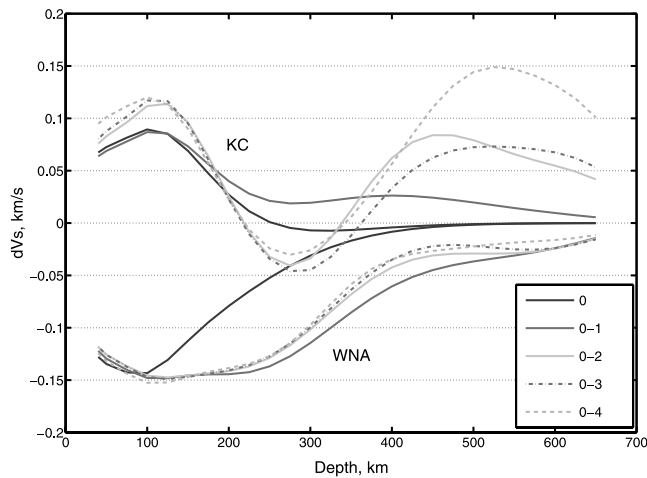


Figure 5. Differences (δV_s) between the starting shear velocity model (see caption for Figure 4) and shear velocity profiles obtained by inverting: mode 0 only (thick solid line), modes 0–1 (thin solid line), modes 0–2 (grey line), modes 0–3 (black dashed line), modes 0–4 (grey dashed line). Note that the shear velocity below 100 km depth is primarily constrained by the overtone data in WNA. The variability in the KC shear velocity profiles at depths larger than 400 km for the data subsets suggests inconsistencies of the high rank overtone data in this region.

ities comparable to those in the 3D model inferred from *Debayle et al.* [2005]. The velocity structure is also similar to the structure constrained by *Li and Burke* [2006] from fundamental mode Rayleigh wave analysis. In agreement with these authors we may therefore infer that the lithospheric keel beneath southern Africa is about 180 km thick. In the WNA profile the very low (<4.3 km/s) shear-wave velocities we observed at depths 50–200 km can be attributed to a low velocity ‘asthenosphere’ beneath western North America, similar to that seen beneath the oceanic lithosphere.

[10] Taking into account the a posteriori errors of our models (Figure 4), we conclude that there is no resolvable shear-velocity difference between the KC and WNA profiles at depths 300–400 km. The WNA velocities are smaller than those inferred from the 3D model of *Debayle et al.* [2005] but model resolution at these depths is better in our study. The lower shear-wave velocities we resolve may simply reflect the presence of the 410 km discontinuity which is absent from our common smooth starting model.

[11] At depths larger than 400 km, the WNA profile follows closely the smoothed PREM starting model while the KC profile exhibits a large 0.15 km/s positive anomaly. We suspect that this feature of the KC model is poorly constrained and that the error bars are underestimated. Indeed, the shear velocity below 400 km depth is mainly constrained by the fourth overtone and, to a lesser extent, by the second overtone (Figure 5). The instability of the inverted velocity profiles beneath KC in this depth-range when subsets of phase velocity data are inverted, suggest that the high-rank ($p > 1$) overtone data are of poor quality. Moreover, receiver function observations from the Kaapvaal craton [*Wittlinger and Farra*, 2007] are inconsistent with the presence of large high shear-wave velocities in the

transition zone, reinforcing our doubt on the quality of mode 2 to 4 observations in KC (Figure 4).

4. Conclusions

[12] New phase velocity measurements from array analysis of regional broadband network data provide new constraints on the average shear velocity structure in western North America and the Kaapvaal Craton region. Fundamental-mode and overtone Rayleigh waves at periods longer than 25 s are recorded coherently over 2000 km distances. U-C diagrams indicate clear mode excitation up to the fourth overtone. 1D shear velocity profiles, representing the average shear velocity structure in the upper mantle, confirm the high shear velocity contrast in the uppermost 150 km of the mantle seen in long-wavelength global models of shear velocity with similar lateral resolution. In addition, our Western North American and Kaapvaal Craton data are explained well by PREM’s velocity structure below a depth of about 400 km. Dismissing the 4th overtone data for the Kaapvaal region, error estimates, suggest that the shear velocity difference cannot exceed 0.1 km/s without compromising data fit at depth larger than 400 km. This robust constraint, due to higher mode phase velocity measurements, places a limit on permissible theoretical shear velocity differences determined from mineralogical and/or thermal models beneath these very different tectonic environments.

[13] **Acknowledgments.** We thank Gérard Wittlinger and Benoit Tauzin for helpful discussions when using their receiver-functions observations. Valuable comments by two anonymous reviewers helped us to improve this paper. Data were provided by the IRIS/DMC. JR acknowledges support from the NSF via EAR-0609763.

References

- Cara, M. (1976), Observation d’ondes Sa de type SH, *Pure Appl. Geophys.*, *114*, 141–157.
- Cara, M., and B. Minster (1981), Multimode-analysis of Rayleigh-type Lg. part 1. Theory and applicability of the method, *Bull. Seismol. Soc. Am.*, *71*, 973–984.
- Carlson, R. W., T. L. Grove, M. J. de Wit, and J. J. Gurney (1996), Anatomy of an Archean craton: A program for interdisciplinary studies of the Kaapvaal craton, southern Africa, *Eos Trans. AGU*, *77*, 273.
- Debayle, E., and J. J. L  v  que (1997), Upper mantle heterogeneities in the Indian Ocean from waveform inversion, *Geophys. Res. Lett.*, *24*, 245–248.
- Debayle, E., B. Kennett, and K. Priestley (2005), Global azimuthal seismic anisotropy and the unique plate-motion deformation of Australia, *Nature*, *433*, 509–512.
- Dziewonski, A. M., and D. L. Anderson (1981), Preliminary reference Earth model, *Phys. Earth Planet. Inter.*, *25*, 297–357.
- Freybourger, M., J. B. Gaherty, and T. H. Jordan (2001), Structure of the Kaapvaal craton from surface waves, *Geophys. Res. Lett.*, *28*, 2489–2492.
- Holschneider, M., M. S. Diallo, M. Kulesh, M. Ohrmberger, E. L  ck, and F. Scherbaum (2005), Characterization of dispersive surface waves using continuous wavelet transforms, *Geophys. J. Int.*, *163*, 463–478.
- L  v  que, J. J., M. Cara, and D. Roulard (1991), Waveform inversion of surface wave data: Test of a new tool for systematic investigation of upper mantle structures, *Geophys. J. Int.*, *104*, 565–581.
- Li, A., and K. Burke (2006), Upper mantle structure of southern Africa from Rayleigh wave tomography, *J. Geophys. Res.*, *111*, B10303, doi:10.1029/2006JB004321.
- Nolet, G. (1975), Higher Rayleigh modes in western Europe, *Geophys. Res. Lett.*, *2*, 60–62.
- Nolet, G. (1990), Partitioned waveform inversion and two-dimensional structure under the network of autonomously recording seismographs, *J. Geophys. Res.*, *95*, 8499–8512.
- Ritsema, J., H. J. van Heijst, and J. H. Woodhouse (2004), Global transition zone tomography, *J. Geophys. Res.*, *109*, B02302, doi:10.1029/2003JB002610.

- Sieminski, A., E. Debayle, and J. J. L ev eque (2003), Seismic evidence for deep low-velocity anomalies in the transition zone beneath West Antarctica, *Earth Planet. Sci. Lett.*, *216*, 645–661.
- Takeuchi, H., and M. Saito (1972), Seismic surface waves, in *Seismology: Surface Waves and Earth Oscillations*, edited by B. A. Bolt, *Methods Comput. Phys.*, *11*, 217–295.
- Tarantola, A., and B. Valette (1982), Generalized nonlinear inverse problem solved using the least squares criterion, *Rev. Geophys.*, *20*, 219–232.
- Trampert, J., H. Paulssen, A. van Wettum, J. Ritsema, R. Clayton, R. Castro, C. Rebolgar, and A. Perez-Vertti (2003), New array monitors seismic activity near the Gulf of California in Mexico, *Eos Trans. AGU*, *84*(4), 29.
- Wittlinger, G., and V. Farra (2007), Converted waves reveal a thick and layered tectosphere beneath the Kalahari super craton, *Earth Planet. Sci. Lett.*, *254*(3–4), 404–415.
- Woodhouse, J. H., and A. M. Dziewonski (1984), Mapping the upper mantle: Three dimensional modeling of Earth structure by inversion of seismic waveforms, *J. Geophys. Res.*, *89*, 5953–5986.

M. Cara, S. Merrer, and L. Rivera, Institut de Physique du Globe de Strasbourg, CNRS and Universit e Louis Pasteur, Strasbourg F-67084, France. (sopie.merrer@eost.u-strasbg.fr)

J. Ritsema, Department of Geological Sciences, University of Michigan, Ann Arbor, MI 48109, USA.